Continuum Electrostatics for Electronic Structure Calculations in Bulk Amorphous Polymers: Application to Polylactide

James H. McAliley, Christopher P. O'Brien, and David A. Bruce*

Department of Chemical and Biomolecular Engineering, Clemson University, Clemson, South Carolina 29634-0909

Received: December 27, 2007; Revised Manuscript Received: May 21, 2008

The bond rotational energy landscapes of polylactide (PLA) oligomers were estimated using electron density functional theory (DFT) at the B3LYP/6-31G** level, both in vacuo and with a self-consistent reaction field (SCRF) method to simulate the electronic environment within the condensed phase. The SCRF method was evaluated for application to polymeric systems, and we demonstrate the difficulties involved in applying the method to bulk amorphous polymers with specific attention to the selection of the solvent probe radius. In addition, rotational isomeric states (RIS) calculations were performed, showing the effect of accounting for the bulk phase reaction field on the bond rotational energetics and characteristic ratio. We conclude that present methods of accounting for bulk environments in electronic structure calculations are not well suited for use with polymeric systems, and the development of improved methods is needed in this area.

Introduction

Although the potential energy surfaces of polymers have often been estimated using the methods of quantum computational chemistry, studies are typically performed in vacuo, without taking into account the effects of interaction with the environment in which the polymer chain is immersed. Such "gas phase" calculations have been applied with generally good success for parametrizing intramolecular interactions in classical force field descriptions of large molecules, especially in cases where the assumed intermolecular parameters are of good quality.[1] However, for other calculations, such as rotational isomeric states (RIS) calculations, the energy landscape must be accurately estimated within the condensed environment to obtain meaningful results. In this paper, we examine the suitability of conventional self-consistent reaction field (SCRF) methods for emulating bulk polymer environments.

In the biomolecular field, the environment surrounding a macromolecule is often a liquid solvent (water), and continuum solvation models have been successfully applied in estimating potential energy barriers to bond rotation in protein chains.[2] For polymeric materials in the bulk, however, the environment encountered by a chain is markedly different from ordinary liquids due to the larger size and reduced mobility of the surrounding polymer chains. Thus, efforts to successfully use conventional dielectric continuum models to describe the bulk amorphous polymer phase must take into account those factors unique to polymer systems. These include size effects on the first "solvation" shell as well as the reduced entropy due to the incorporation of the solvating units into larger chains.

In this study, the polymer of interest is polylactide, also called poly(lactic acid) or PLA. This is a polymer with a relatively low dielectric constant, and it is currently of practical interest to many researchers due to its environmental benefits.[3] PLA can be produced commercially from corn feedstocks, with an overall consumption of carbon dioxide, and at the end of its useful life may be composted and fully biodegrades into ecologically benign components.[4]

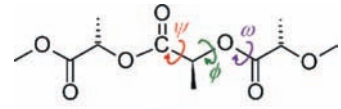

1

Figure 1. Methyl terminated L-lactic acid trimer used in determining bond rotational potentials. Dihedrals ϕ and Ψ are the principle degrees of freedom studied.

Computations were performed on oligomeric surrogates of PLA using electron density functional theory (DFT), both in vacuo and within a simulated bulk phase. On the basis of these results, RIS calculations were performed for comparison with experimental (viscometric) measurements of the unperturbed chain dimensions of PLA. In this work, we demonstrate that the application of a continuum electrostatic model can have a dramatic effect on estimating bond rotational behavior of polymers, and we discuss the difficulties involved in applying such models to polymer systems.

Methods

The quantum mechanical results detailed in this work were generated using Jaguar 4.2 software[5] on a Beowulf cluster comprising 160 dual-CPU (997 MHz Pentium III) nodes running Linux kernel 2.6.8. All computations were based upon DFT at the B3LYP/6-31G** level, which was chosen due to its computational efficiency and its wide usage and availability. Though it should be mentioned that recent publications have highlighted the shortcomings of this functional/basis set, especially in estimating dispersion interactions,[6,7] this level of theory has previously been shown to perform well when estimating bond rotational energy barriers of small organic molecules.[8]

Computations were carried out on conformations of molecule **1** (Figure 1) having varying bond rotations, where we have adopted nomenclature commonly used in the protein literature to identify main chain torsional coordinates. Thus, the principal bond rotational degrees of freedom within the central lactyl

* E-mail: dbruce@clemson.edu.

10.1021/jp712114q CCC: $40.75
Published on Web 07/16/2008

repeat unit of **1** are labeled in Figure 1 as ϕ and Ψ, with these dihedral angles defined by the IUPAC convention[9] and using the coordinates of main-chain, or "backbone" atoms. The main-chain bond rotation between the carbonyl carbon and the ester oxygen, labeled ω, has often been shown to reside solely in its *trans* energy basin, and our calculations confirm this with a potential energy barrier of nearly 60 kJ/mol. Thus, the conformational space associated with all values of ω was not investigated because much of these conformations would be energetically unfavored at temperatures where the polymer is chemically stable. The ends of molecule **1** have been terminated with methyl groups to avoid hydrogen bonding interactions initially observed in the hydroxy acid version of the molecule.

In generating the bond rotational energy surfaces shown in this work, a sequential grid search was used, starting with several unique conformations of molecule **1**. These unique conformations were identified after unconstrained energy minimization of 144 input structures, with ϕ and Ψ varied at 30° increments. In general, for each choice of solvation environment, only a small number (5−7) of unique stationary points were identified. Starting from the geometries of these stationary points, the values of ϕ and Ψ were perturbed at 5° increments, and constrained energy minimizations were performed with ϕ and Ψ held constant. These optimized geometries were in turn perturbed at 5° increments in ϕ and Ψ, and the process was continued until a diagonal grid of 2592 (ϕ, Ψ) points was obtained. Though this is certainly a large number of geometry optimizations, the small bond rotations of 5° resulted in fewer optimization steps needed per input structure, and computationally it was as efficient or more so than using a coarser grid. Further, the finer grid allowed us to more accurately define the values of the true energy minima on the (ϕ, Ψ) surface. Because the grid search was carried out using several starting points, the lowest energy structure is reported at each point on the (ϕ, Ψ) grid.

Calculations in Vacuo. The standard B3LYP functionals were used in Jaguar 4.2[5] for the estimation of properties in vacuo. Zero point energy corrections were not applied, as the calculated normal mode vibrations are nearly equal for the different conformers studied and, thus, are not important when considering the relative energy difference between conformers.

Calculations in the Bulk Amorphous Phase. Calculation of condensed phase properties via electronic structure methods has been discussed extensively in the literature, and for a comprehensive review the reader is directed to the papers of Tomasi and Persico[10] and Cramer and Truhlar.[11] Though such methods have been extended for solvents as large as *n*-hexadecane,[12] these techniques have not been applied to model amorphous polymer environments. In the present work, we utilize the self-consistent reaction field (SCRF) method as implemented in Jaguar version 4.2.[5] The principal adjustable parameters in this method are the internal dielectric constant within the cavity, ϵ_{in}, the dielectric constant of the continuum outside the cavity, ϵ_{out}, and the probe radius, r_p, defining the size of the molecular cavity (see ref 13). Because the electronic wave function is solved explicitly for the molecule within the cavity, it is customary to use a value of $\epsilon_{in} = 1.0$, and because the dielectric constant of PLA has been measured experimentally, we set $\epsilon_{out} = 2.83$ for PLA at room temperature.[14] However, the choice of a proper probe radius is not as obvious.

When the solvation effects of small molecules are of interest, the probe radius parameter has a meaningful definition, namely, one-half the thickness of the first solvation shell surrounding the solute molecule. Thus, it is on the order of the solvent's molecular dimensions. In the case of small solvent molecules of approximately spherical geometry, r_p is easily estimated from knowledge of the size and packing of the solvent molecules.[15]

$$r_p^3 = \frac{3m\Delta}{4\pi\rho} \tag{1}$$

Here, m represents the mass of a single solvent molecule, Δ is the packing density, and ρ is the (bulk) density of the solvent. Typical values of probe radii used for solvation calculations are between 1 and 3 Å. The approximation of spherical solvent geometries implicit in eq 1 has been shown to work well in cases where all length dimensions of the solvent are on the same order of magnitude. However, for solvation of oligomers in a high molecular weight polymer matrix, relating the size of the first solvation shell to the solvent molecular dimensions is difficult because the length of a polymer chain can be orders of magnitude larger than its width.

When dealing with the solvation effects of the bulk polymer phase, we have identified several probe radii that may be considered characteristic of the bulk medium. First is the length scale of a lactyl unit ($CHCH_3OCO$), or, from eq 1, about 2.28 Å (assuming a packing density of 0.5). Another estimate for the probe radius can be obtained using solvents with similar functionality and dielectric constant to PLA, such as diethyl carbonate. Using accepted packing densities for this solvent[16] and eq 1, one calculates the probe radius to be 2.83 Å. Yet another reasonable estimate of the probe radius may be arrived at by considering the polymer under Flory Θ-conditions, defined as the solvent composition and temperature at which a polymer solute has equal interactions with itself and with its solvent. It has been estimated that dibutyl phthalate and dipropyl phthalate are Θ-solvents for pure isotactic PLA at approximately 80 and 0 °C, respectively.[17] Using eq 1 for these solvents, probe radii are found to be approximately 9 and 11 Å, respectively. We note that these are, of course, *extremely* large values for use in SCRF methods. Because the SCRF continuum is purely electrostatic in nature, a cavity of this size would presumably yield results similar to those of in vacuo calculations. In practice, we found that the Poisson−Boltzmann solver failed to converge when using probe radii larger than 8 Å; therefore, this was the largest probe radius examined. In addition, a probe radius of 5 Å was considered as an intermediate between the size of a repeat unit and the Θ-solvents.

As the focus of this paper is only on quantifying the relative energies associated with bond rotation, and not absolute solvation energies, we have neglected the nonpolar cavity term in reporting energy landscapes in the condensed phase.

Partial Atomic Charges. The assignment of partial atomic charges influences the quality of the SCRF calculations. In estimating charges during SCRF calculations, the total charge and dipole moment were replicated in the ESP fit, and Jaguar's default (spherical) grid spacing was used.

Rotational Isomeric State (RIS) calculations. The RIS method was used to estimate unperturbed chain dimensions of amorphous PLA. In this work, two different RIS methods were utilized. In the first, we adopt the virtual bond definitions for PLA as originally laid out by Flory.[18–20] The characteristic ratio for this system can be obtained analytically by the relation[19]

$$C_{\infty,v} = \{(\mathbf{I} + \langle \mathbf{T} \rangle)(\mathbf{I} - \langle \mathbf{T} \rangle)^{-1}\}_{11} \tag{2}$$

where $\mathbf{I}$ is the identity matrix of order three, $\langle \mathbf{T} \rangle$ is the ensemble-averaged transition matrix, and the desired matrix element {1, 1} is given by the subscript. The subscript v indicates the basis of virtual bonds. For a particular geometry, the matrix $\mathbf{T}$ can

be expressed as a product of three matrices, $\mathbf{T}^{\xi}\mathbf{T}^{\theta\phi}\mathbf{T}^{\eta\Psi}$. The reader is referred to the previously cited works of Flory and co-workers for an in-depth explanation of the method, including definitions of the geometric parameters. However, we note that the dihedral angle convention used in those references is opposite to the IUPAC convention used in this work. Thus, using the IUPAC convention for ϕ and Ψ, the transition matrices are computed by

$$\mathbf{T}^{\theta\phi} = \begin{bmatrix} \cos\theta & \sin\theta & 0 \\ -\sin\theta\cos\phi & \cos\theta\cos\phi & -\sin\phi \\ -\sin\theta\sin\phi & \cos\theta\sin\phi & \cos\phi \end{bmatrix} \quad (3)$$

and

$$\mathbf{T}^{\eta\Psi} = \begin{bmatrix} \cos\eta & -\sin\eta & 0 \\ -\sin\eta\cos\Psi & -\cos\eta\cos\Psi & \sin\Psi \\ -\sin\eta\sin\Psi & -\cos\eta\sin\Psi & -\cos\Psi \end{bmatrix} \quad (4)$$

The matrix $\mathbf{T}^{\xi}$ remains the same as given by Flory. This method relies on the explicit assumption that ω remains constant at exactly 180° in each repeat unit, regardless of the value of ϕ and Ψ. As discussed in the Results and Discussion, this assumption is invalid as the actual value of the ω dihedral deviates slightly from 180° to reduce other high-energy interactions within the molecule.

To circumvent the artificial constraint of ω at 180° in Flory's analytical method, we have employed a Monte Carlo method as a second approach to obtaining the amorphous statistics from the RIS model. With this method, the (ϕ, Ψ) parameter space is sampled according to a Boltzmann distribution, and chains are constructed by reading the bond lengths, valence angles, and dihedral angles for the backbone atoms directly from the **z**-matrix output of the DFT calculations associated with those sampled values of ϕ and Ψ. All geometric parameters were taken from the central repeat unit of molecule **1**. Although this method accounts for variations in molecular geometry, it is susceptible to statistical uncertainty due to incomplete sampling of phase space. In practice, several million Monte Carlo iterations were needed before converging on a meaningful estimate.

To allow for a more straightforward comparison of analytical and Monte Carlo RIS results to those reported in the literature, we report all analytical estimates of the characteristic ratio on the basis of real bonds,

$$C_{\infty} = C_{\infty,\mathrm{v}}\frac{l_{\mathrm{v}}^{2}}{n_{\mathrm{r/v}}l^{2}} \quad (5)$$

where l_{v} is the average length of a virtual bond, $n_{\mathrm{r/v}}$ is the number of real bonds per virtual bond, and l is the average length of a real bond. By definition, $n_{\mathrm{r/v}}$ is 3 for PLA, and we use the average squared real bond length of 2.05 Å^2 as adopted by Dorgan.[21] For each SCRF probe radius, as well as for the gas phase, the mean squared virtual bond length was calculated using a Boltzmann-weighted average over all structures in the appropriate composite rotational energy surface.

Results and Discussion

Rotations about ϕ and Ψ. Potential energy surfaces for bond rotations of molecule **1** about ϕ and Ψ in the gas phase and using the SCRF method (with several different probe radii) are shown in Figure 2. The suitability of each potential energy surface for describing bulk PLA can be best determined by examining features of the energy landscapes. The general topologies of the energy landscapes in Figure 2 are all similar to each other, though markedly different than the commonly cited energy landscape put forth by Brant, Tonelli, and Flory,[20]

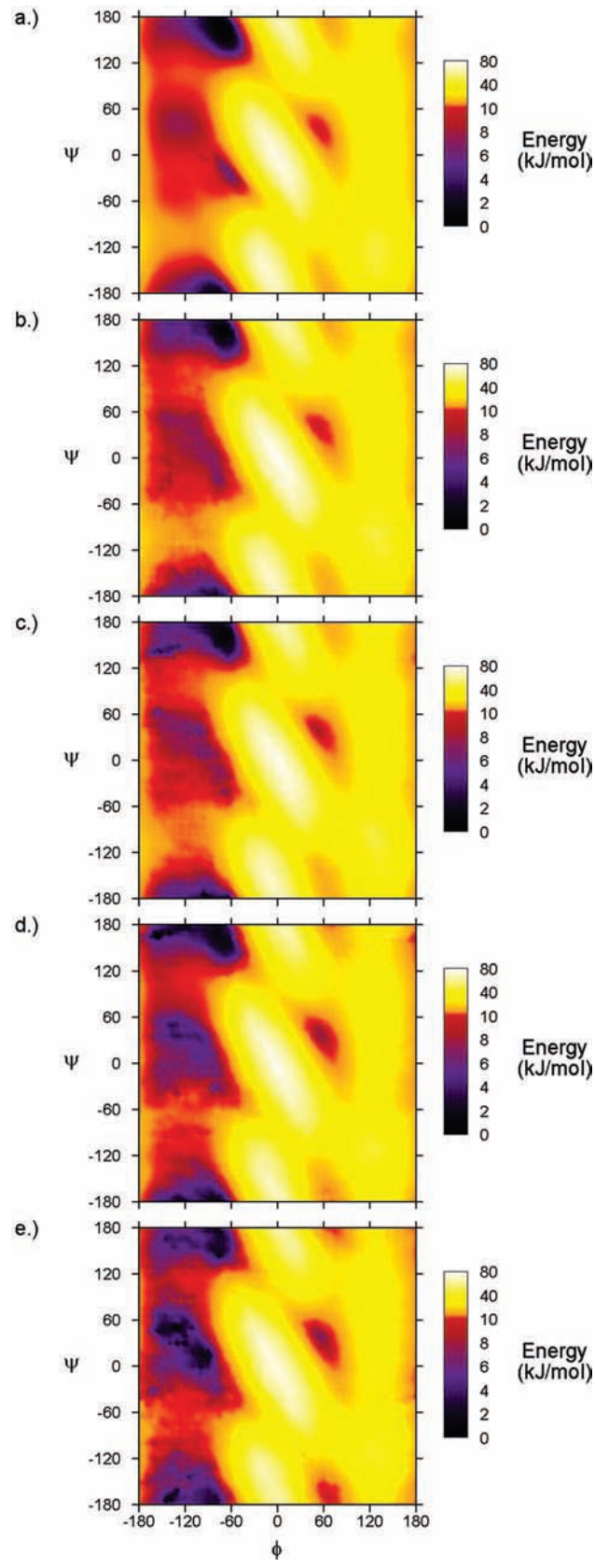

Figure 2. Bond rotational energy profiles for the ϕ and Ψ dihedrals of molecule 1. Plot a shows in vacuo calculations; plots b−e were obtained with the SCRF method, using a probe radius of (b) $r_{\mathrm{p}} = 2.28$, (c) $r_{\mathrm{p}} = 2.83$, (d) $r_{\mathrm{p}} = 5.00$, and (e) $r_{\mathrm{p}} = 8.00$. In each plot, energies are shifted such that the lowest energy point is assigned a value of zero.

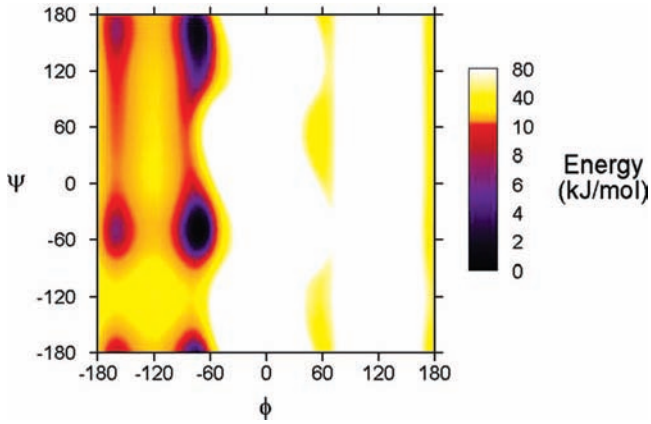

Figure 3. Bond rotational energy surface constructed with the van der Waals model and point-charge electrostatics as described by Flory and others.[20] IUPAC dihedral angle conventions are used. White space denotes regions that are greater than or equal to 80 kJ/mol.

as shown in Figure 3. In their model, the potential energy surface is dominated by four distinct minima corresponding to structures having IUPAC (ϕ, Ψ) values of (−73, −46), (−73, 158), (−160, −50), and (−160, 161). Here we denote these minimum energy conformers as g^-c, g^-t, tc, and tt, respectively, with g representing *gauche*, c representing *cis*, and t representing *trans*. Although the DFT energy surfaces in Figure 2 show the low-energy regions of Figure 3 to be generally accessible, the four sharply distinct minima in Flory's model are not observed. Rather, the DFT results show two very broad basins in the $g-t$ and g^-c regions, enveloping one or more loosely connected local minima depending on the solvation parameters used. In general, these local minima within the larger basins are not separated by the distinct energy barriers reported by Brant, Tonelli, and Flory.[20] In addition, the DFT results show the two local minima where ϕ takes on a g^+ conformation to be lower in energy than predicted by Flory's semiempirical model. Still, the energies of the g^-t and g^-c basins are such that they render contributions from the minor g^+t and g^+c minima to be negligibly important.

Although there is little difference in the overall topology of the DFT-derived energy surfaces, we do observe a general trend in the relative energies of the g^-t and g^-c basins as the solvent probe radius is increased. The g^-t basin, near ($\phi = -70°$, $\Psi = 162°$), represents the minimum energy structure for all simulation conditions but the highest SCRF probe radius examined, with the g^-c becoming progressively more stable as r_p is increased. In terms of chain conformations, the g^-c basin corresponds to a 4_1 helix, and the g^-t basin is in the vicinity of the 10_3 helical residues associated with the most stable crystalline form of PLA ($\phi = -64.2°$, $\Psi = 155.7$, when averaged over the 5 residues in the α-form proposed by Sasaki and Asakura;[22] for pictorial representations of these conformations, the reader is referred to Figure 3 of Meaurio et al.[23]). When considering the relative stabilities of g^-t and g^-c, one might expect the g^-t basin to be the global minimum because it corresponds to the most stable crystalline structure. However, comparison based on crystal structure data is ill-advised, because the SCRF method is intended for use only in isotropic bulk phases. Thus, to evaluate the suitability of the SCRF model in this application, we modeled the properties of PLA in the disordered amorphous state rather than the crystalline phase.

One peculiarity shown in the data warrants some discussion, and that is the direction of the trend observed with respect to the probe radius in the SCRF calculations. One would expect the larger probe radii to more closely resemble gas phase behavior; however, it is the largest probe radius that shows the highest deviations in relative energies of the g^-t and g^-c basins, when compared to in vacuo calculations. Because the SCRF method is based solely on electrostatic interactions, one would expect a cavity of this size to have little or no influence on the electronic structure calculation. It should be emphasized that this subtlety only applies to the trend in *relative* energies of basins on the same potential energy surface, whereas the absolute energies follow the expected trend as shown in Table 1 (absolute energies become closer to those for the in vacuo calculations as r_p is increased).

TABLE 1: Absolute Energies of the Lowest Energy g^-t Minima Found during Unconstrained Minimization of Molecule 1

solvation treatment	ϕ (deg)	Ψ (deg)	energy (hartrees)
r_p =2.28Å	−79.6	169.6	−206467.4
r_p =2.83Å	−77.1	167.2	−206465.3
r_p =5.00Å	−79.5	167.3	−206460.6
r_p =8.00Å	−76.6	163.1	−206455.6
in vacuo	−70.1	161.3	−206396.4

RIS Calculations. Amorphous chain dimensions were obtained using RIS calculations as described in the Methods. Upon an increase in the SCRF probe radius used in DFT simulations, the progressive stabilization of PLA conformations contained in the g^-c potential energy basin relative to the g^-t basin has the effect of shortening the probable end-to-end distances of the polymer. Conversely, C_∞ becomes larger when chain statistics are dominated by conformations contained in the g^-t rotational energy basin, which correspond to extended helical chains of PLA. Figure 4 shows C_∞ as calculated by Flory's analytical approach, as well as the numerical Monte Carlo scheme. Though the temperature range shown in the figure extends partially into the glassy state of PLA, we assert here that RIS calculations are only valid above the glass transition temperature (T_g). Upon cooling below T_g, the bond rotational states become kinetically trapped, a phenomenon easily seen in Figure 11 of Meaurio et al.,[23] at which point Boltzmann statistics may no longer be assumed. Therefore, to estimate C_∞ of amorphous PLA at room temperature, the appropriate RIS calculation should be carried out at T_g, which can vary from 50

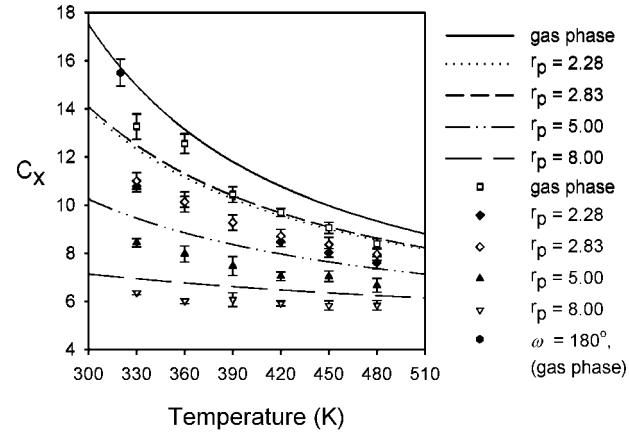

Figure 4. Calculated values of C_∞ from the (ϕ, Ψ) potential energy surfaces shown in Figure 2. Lines represent calculations based on Flory's analytical approach, and symbols represent results of the Monte Carlo approach. Data points were averaged over at least three separate Monte Carlo runs, each with one million sampled configurations. Error bars give the 95% confidence intervals. The data point at 320 K is shown to illustrate the effects of assuming the ester moiety is planar in the Monte Carlo method.

to 80 °C depending on molecular weight, enantiomeric purity, and moisture content.[3]

There is an obvious systematic difference in the calculated C_∞ values from Flory's analytical method and the numerical Monte Carlo approach, and we have shown that this arises from the assumption that ω is a constant 180° for all structures in the Flory model. In the energy minimizations performed in this work, the optimal value of ω was approximately 172° for most energetically accessible conformations, though deviations were observed especially in the high-energy states visited during the conformation searches. Therefore, Flory's analytical method assumes the chain is stiffer than it actually is and, thus, overestimates the value of C_∞. The Monte Carlo approach accounts for deviations in the dihedral angle ω; therefore, it should yield a more accurate estimate of C_∞. As expected, Monte Carlo trials in which ω was set to a constant 180° resulted in values of C_∞ that were nearly equal to that calculated from eq 2, reinforcing our assertion that the assumption of planarity in the ester moiety is responsible for the systematic difference shown in Figure 4. For illustration, one such value obtained at 320 K is shown in Figure 4.

In comparison with previous modeling studies on PLA, the values of C_∞ calculated here are close to or within the range reported by Blomqvist et al.,[24] which was found using an explicit treatment of interactions between the polymer chains and the bulk amorphous environment. Using their force field model, it was found that calculated C_∞ values range from 5.7 to 12.1, depending on the treatment of nonbonded interactions in intrachain segments. The simpler, van der Waals model of Flory and co-workers gives a value of 4.75,[20] which is just outside of the range calculated here.

Experimental values for C_∞ vary widely in the literature.[20,21,25] A recent publication by Dorgan[21] asserts persuasively that the true value is likely close to 6.5, based on intrinsic viscosity data in several different solvents and extensive statistical analysis. In this work, a C_∞ value this low was only calculated using the largest probe radius, 8.00 Å. As previously stated, values of r_p on this order correspond to the spherical molecule approximation of a Θ-solvent for PLA, such as dibutyl phthalate. The idea that the most suitable SCRF probe radius for modeling amorphous polymers should be the size of a Θ-solvent certainly seems enticing. Not only would this protocol be convenient to apply in practice, but it also has an intuitive interpretation that combines the SCRF framework with a fundamental concept of polymer science. However, it should be recognized that the SCRF method was developed and validated for relatively small probe radii, and 8.00 Å is vastly larger than those encountered in conventional SCRF calculations. Though it is understandable that a bulk polymer phase might interact over larger length scales than conventional liquid solvents, a probe radius of 8.00 Å is probably larger than we can justify for use in this model. When one considers the physical ramifications of such a large probe radius—that the interaction of bulk PLA with a solute is equivalent to that of a vacuum for nearly a nanometer in all directions surrounding the solute—it is unlikely that such a model would adequately describe a condensed phase system.

We must also address the inconsistencies in the literature regarding the unperturbed dimensions of PLA. Although Dorgan's publication is most recent, another estimate of C_∞ very commonly encountered in the literature is that of Joziasse,[25] which puts the value at approximately 11.7. It cannot be ignored that this value is more closely reproduced by probe radii on the order of the lactyl unit's size, and thus, would suggest that the proper probe radius is on the order of the chain repeating unit rather than the Θ-solvent. However, given the current state of the literature, accepting either of these assertions about the appropriate probe radius as a general rule would require more rigorous testing on different polymer systems.

Conclusions

Although often neglected in DFT calculations for polymeric materials, we have shown that a treatment of the condensed phase reaction field surrounding a polymer molecule can have a dramatic effect on the calculation of relative conformational energies for use in RIS models. These effects would likely be more significant for polymers with higher dielectric constants than PLA. However, most solvation models for use in ab initio calculations are not well suited for describing a polymeric solvent phase, and in particular we have shown the difficulties involved in selecting a suitable solvent probe radius parameter for use in a conventional SCRF method.

We have demonstrated that accounting for the reaction field allows for improved agreement with recent viscometric data, when compared to conventional DFT calculations in vacuo, but only when using cavity sizes much larger than those with which the SCRF method was designed and validated. Use of such large cavity sizes in the SCRF model does not seem physically reasonable for modeling a condensed phase, and therefore, we cannot recommend such a protocol based solely on this limited study. Rather, it is likely that these results are only indicative of the level of approximation of continuum electrostatic methods in modeling condensed phases, which is manifest in the relatively arbitrary selection of the probe radius parameter.

We believe that the development of more specialized solvation models could further improve the predictive capabilities of electronic structure calculations on molecules in bulk amorphous polymeric environments. It is likely that such models will take the direction suggested by Giesen et al.,[12] where multiple length scales define the solvent cavity to capture the complex interactions between the solute and its polymer environment. We suggest that such a model would need extensive validation based directly on solubilities of small molecules in amorphous polymers, before attempting to predict relative conformational energies as desired in this study.

Acknowledgment. We acknowledge the support of the Center for Advanced Engineering Fibers and Films and the ERC program of the National Science Foundation under Award Number EEC-9731680.

Supporting Information Available: Molecular geometries in Cartesian coordinates are available for all structures reported in Figure 2, along with the energies and partial atomic charges calculated for each conformer. This information is available free of charge via the Internet at http://pubs.acs.org.

References and Notes

(1) Kaminski, G. A.; et al. Evaluation and reparametrization of the OPLS-AA force field for proteins via comparison with accurate quantum chemical calculations on peptides. *J. Phys. Chem. B* **2001**, *105* (28), 6474–6487.

(2) Duan, Y.; et al. A point-charge force field for molecular mechanics simulations of proteins based on condensed-phase quantum mechanical calculations. *J. Comput. Chem.* **2003**, *24* (16), 1999–2012.

(3) Auras, R.; Harte, B.; Selke, S. An overview of polylactides as packaging materials. *Macromol Biosci* **2004**, *4* (9), 835–864.

(4) Sinclair, R. G. The case for polylactic acid as a commodity packaging plastic. *J. Macromol. Sci.-Pure Appl. Chem.* **1996**, *A33* (5), 585–597.

(5) Jaguar 4.2. 1991−2000, Schrodinger, Inc.: Portland, OR.

(6) Wodrich, M. D.; et al. How accurate are DFT treatments of organic energies? *Org. Lett.* **2007**, *9* (10), 1851–1854.

(7) Zhao, Y.; et al. Tests of second-generation and third-generation density functionals for thermochemical kinetics. *Phys. Chem. Chem. Phys.* **2004**, *6* (4), 673–676.

(8) St.-Amant, A.; et al. Calculation of Molecular Geometries, Relative Conformational Energies, Dipole Moments, and Molecular Electrostatic Potential Fitted Charges of Small Organic Molecules of Biochemical Interest by Density Functional Theory. *J. Comput. Chem.* **1995**, *16* (12), 1483–1506.

(9) McNaught, A. D. and Wilkinson A. eds. *Compendium of Chemical Terminology: IUPAC Recommendations*, 2nd ed.; Blackwell Scientific Publications: Oxford, U.K., 1997.

(10) Tomasi, J.; Persico, M. Molecular-Interactions in Solution - an Overview of Methods Based on Continuous Distributions of the Solvent. *Chem. Rev.* **1994**, *94* (7), 2027–2094.

(11) Cramer, C. J.; Truhlar, D. G. Implicit solvation models: Equilibria, structure, spectra, and dynamics. *Chem. Rev.* **1999**, *99* (8), 2161–2200.

(12) Giesen, D. J.; et al. General Semiempirical Quantum-Mechanical Solvation Model for Nonpolar Solvation Free-Energies - N-Hexadecane. *J. Am. Chem. Soc.* **1995**, *117* (3), 1057–1068.

(13) Cortis, C. M.; Friesner, R. A. An automatic three-dimensional finite element mesh generation system for the Poisson-Boltzmann equation. *J. Comput. Chem.* **1997**, *18* (13), 1570–1590.

(14) Kanchanasopa, M.; Runt, J. Broadband dielectric investigation of amorphous and semicrystalline L-lactide/meso-lactide copolymers. *Macromolecules* **2004**, *37* (3), 863–871.

(15) Wright, J. R. Jaguar User's Guide, Version 4.2. 2002: Schrodinger, Inc.

(16) Kodaka, M. Correlation between molecular size and packing density of solvents. *J. Phys. Chem. B* **2004**, *108* (3), 1160–1164.

(17) Lee, J. S.; Lee, H. K.; Kim, S. C. Thermodynamic parameters of poly(lactic acid) solutions in dialkyl phthalate. *Polymer* **2004**, *45*, 4491–4498.

(18) Brant, D. A.; Flory, P. J. The Configuration of Random Polypeptide Chains. II. Theory. *J. Am. Chem. Soc.* **1965**, *87* (13), 2791–2798.

(19) Flory, P. J. *Statistical Mechanics of Chain Molecules*; Wiley: New York, 1989.

(20) Brant, D. A.; Tonelli, A. E.; Flory, P. J. The Configurational Statistics of Random Poly(lactic acid Chains. II. Theory. *Macromolecules* **1969**, *2* (3), 228–235.

(21) Dorgan, J. R.; et al. Fundamental solution and single-chain properties of polylactides. *J. Polym. Sci. Part B-Polym. Phys.* **2005**, *43* (21), 3100–3111.

(22) Sasaki, S.; Asakura, T. Helix distortion and crystal structure of the alpha-form of poly(L-lactide). *Macromolecules* **2003**, *36* (22), 8385–8390.

(23) Meaurio, E.; et al. Conformational behavior of poly(L-lactide) studied by infrared spectroscopy. *J. Phys. Chem. B* **2006**, *110* (11), 5790–5800.

(24) Blomqvist, J. RIS Metropolis Monte Carlo studies of poly(L-lactic), poly(L,D-lactic) and polyglycolic acids. *Polymer* **2001**, *42* (8), 3515–3521.

(25) Joziasse, C. A. P.; et al. On the chain stiffness of poly(lactide)s. *Macromol. Chem. Phys.* **1996**, *197* (7), 2219–2229.

JP712114Q